# The hidden anatomy of paranasal sinuses reveals biogeographically distinct morphotypes in the ninebanded armadillos (*Dasypus novemcinctus*) (#17199)

First submission

Please read the **Important notes** below, the **Review guidance** on page 2 and our **Standout reviewing tips** on page 3. When ready **submit online**. The manuscript starts on page 4.

### Important notes

#### **Editor and deadline**

Laura Wilson / 29 Apr 2017

**Files** 7 Figure file(s)

1 Table file(s)

1 Raw data file(s)

Please visit the overview page to **download and review** the files

not included in this review PDF.

**Declarations**No notable declarations are present



Please read in full before you begin

### How to review

When ready <u>submit your review online</u>. The review form is divided into 5 sections. Please consider these when composing your review:

- 1. BASIC REPORTING
- 2. EXPERIMENTAL DESIGN
- 3. VALIDITY OF THE FINDINGS
- 4. General comments
- 5. Confidential notes to the editor
- 1 You can also annotate this PDF and upload it as part of your review

To finish, enter your editorial recommendation (accept, revise or reject) and submit.

#### **BASIC REPORTING**

- Clear, unambiguous, professional English language used throughout.
- Intro & background to show context.
  Literature well referenced & relevant.
- Structure conforms to **PeerJ standards**, discipline norm, or improved for clarity.
- Figures are relevant, high quality, well labelled & described.
- Raw data supplied (see **PeerJ policy**).

#### **EXPERIMENTAL DESIGN**

- Original primary research within **Scope of** the journal.
- Research question well defined, relevant & meaningful. It is stated how the research fills an identified knowledge gap.
- Rigorous investigation performed to a high technical & ethical standard.
- Methods described with sufficient detail & information to replicate.

#### **VALIDITY OF THE FINDINGS**

- Impact and novelty not assessed.
  Negative/inconclusive results accepted.
  Meaningful replication encouraged where rationale & benefit to literature is clearly stated.
- Data is robust, statistically sound, & controlled.
- Conclusions are well stated, linked to original research question & limited to supporting results.
- Speculation is welcome, but should be identified as such.

The above is the editorial criteria summary. To view in full visit <a href="https://peerj.com/about/editorial-criteria/">https://peerj.com/about/editorial-criteria/</a>

### 7 Standout reviewing tips



The best reviewers use these techniques

	n
	N

## Support criticisms with evidence from the text or from other sources

### Give specific suggestions on how to improve the manuscript

### Comment on language and grammar issues

### Organize by importance of the issues, and number your points

### Give specific suggestions on how to improve the manuscript

## Please provide constructive criticism, and avoid personal opinions

## Comment on strengths (as well as weaknesses) of the manuscript

### **Example**

Smith et al (J of Methodology, 2005, V3, pp 123) have shown that the analysis you use in Lines 241-250 is not the most appropriate for this situation. Please explain why you used this method.

Your introduction needs more detail. I suggest that you improve the description at lines 57-86 to provide more justification for your study (specifically, you should expand upon the knowledge gap being filled).

The English language should be improved to ensure that your international audience can clearly understand your text. I suggest that you have a native English speaking colleague review your manuscript. Some examples where the language could be improved include lines 23, 77, 121, 128 - the current phrasing makes comprehension difficult.

- 1. Your most important issue
- 2. The next most important item
- 3. ...
- 4. The least important points

Line 56: Note that experimental data on sprawling animals needs to be updated. Line 66: Please consider exchanging "modern" with "cursorial".

I thank you for providing the raw data, however your supplemental files need more descriptive metadata identifiers to be useful to future readers. Although your results are compelling, the data analysis should be improved in the following ways: AA, BB, CC

I commend the authors for their extensive data set, compiled over many years of detailed fieldwork. In addition, the manuscript is clearly written in professional, unambiguous language. If there is a weakness, it is in the statistical analysis (as I have noted above) which should be improved upon before Acceptance.



# The hidden anatomy of paranasal sinuses reveals biogeographically distinct morphotypes in the nine-banded armadillos (*Dasypus novemcinctus*)

Guillaume Billet Corresp., 1, Lionel Hautier 2, Benoit de Thoisy 3, Frédéric Delsuc 2

Corresponding Author: Guillaume Billet Email address: guillaume.billet@mnhn.fr

Background. With their Pan-American distribution, long-nosed armadillos (genus Dasypus) constitute an understudied model for Neotropical biogeography. This genus currently comprises seven recognized species, the nine-banded armadillo (D. novemcinctus) having the widest distribution ranging from Northern Argentina to the South-Eastern US. With their broad diversity of habitats, nine-banded armadillos provide a useful model to explore the effects of climatic and biogeographic events on morphological diversity at a continental scale.

Methods. Based on a sample of 136 skulls of Dasypus spp., including 112 specimens identified as D. novemcinctus, we studied the diversity and pattern of variation of internal paranasal cavities, which were reconstructed virtually using  $\mu$ CT-scanning or observed through bone transparency.

Results. Our qualitative analyses of paranasal sinuses and recesses successfully retrieved a taxonomic differentiation between the traditional species D. kappleri, D. pilosus and D. novemcinctus but failed to recover diagnostic features between the disputed and morphologically similar D. septemcinctus and D. hybridus. Most interestingly, the high variation detected in our large sample of D. novemcinctus showed a clear geographical patterning, with the recognition of three well-separated morphotypes: one ranging from North and Central America and parts of northern South America west of the Andes, one distributed across the Amazonian Basin and central South America, and one restricted to the Guiana Shield.

Discussion. The question as to whether these paranasal morphotypes may represent previously unrecognized species is to be evaluated through a thorough revision of the Dasypus species complex integrating molecular and morphological data. Remarkably, our recognition of a distinct morphotype in the Guiana Shield area is congruent with the recent discovery of a divergent mitogenomic lineage in French Guiana. The inflation of the second medialmost pair of caudal frontal sinuses constitutes an unexpected morphological diagnostic feature for this potentially distinct species. Our results demonstrate the benefits of studying overlooked internal morphological structures in supposedly cryptic species revealed by molecular data. It also illustrates the under-exploited potential of the highly variable paranasal sinuses of armadillos for systematic studies.

<sup>1</sup> Sorbonne Universités, CR2P, UMR 7207, CNRS, Université Paris 06, Museum national d'Histoire naturelle, Paris, France

<sup>&</sup>lt;sup>2</sup> Institut des Sciences de l'Evolution, UMR 5554, CNRS, IRD, EPHE, Université de Montpellier, Montpellier, France

<sup>3</sup> Institut Pasteur de la Guyane, Cayenne, French Guiana



6

13

16

- 1 The hidden anatomy of paranasal sinuses reveals biogeographically
- 2 distinct morphotypes in the nine-banded armadillos (Dasypus
- 3 novemcinctus)
- 5 Guillaume BILLET<sup>1</sup>, Lionel HAUTIER<sup>2</sup>, Benoit de THOISY<sup>3,4</sup>, and Frédéric DELSUC<sup>2</sup>
- <sup>1</sup>Sorbonne Universités, CR2P, UMR 7207, CNRS, Université Paris 06, Muséum national
- 8 d'Histoire naturelle, Paris, France.
- 9 <sup>2</sup>Institut des Sciences de l'Evolution, UMR 5554, CNRS, IRD, EPHE, Université de Montpellier,
- 10 Montpellier, France.
- <sup>3</sup>Institut Pasteur de la Guyane, BP 6010, 97300 Cayenne, French Guiana.
- <sup>4</sup>Association Kwata, BP 672, 97300 Cayenne, French Guiana.
- 14 Corresponding Author
- 15 Guillaume BILLET, guillaume.billet@mnhn.fr
- 17 Abstract
- 18 **Background.** With their Pan-American distribution, long-nosed armadillos (genus *Dasypus*)
- 19 constitute an understudied model for Neotropical biogeography. This genus currently comprises
- seven recognized species, the nine-banded armadillo (D. novemcinctus) having the widest
- 21 distribution ranging from Northern Argentina to the South-Eastern US. With their broad



diversity of habitats, nine-banded armadillos provide a useful model to explore the effects of 22 climatic and biogeographic events on morphological diversity at a continental scale. 23 **Methods.** Based on a sample of 136 skulls of *Dasypus* spp., including 112 specimens identified 24 as D. novemcinctus, we studied the diversity and pattern of variation of internal paranasal 25 cavities, which were reconstructed virtually using µCT-scanning or observed through bone 26 27 transparency. **Results.** Our qualitative analyses of paranasal sinuses and recesses successfully retrieved a 28 29 taxonomic differentiation between the traditional species D. kappleri, D. pilosus and D. novemcinctus but failed to recover diagnostic features between the disputed and morphologically 30 31 similar D. septemcinctus and D. hybridus. Most interestingly, the high variation detected in our large sample of D. novemcinctus showed a clear geographical patterning, with the recognition of 32 three well-separated morphotypes: one ranging from North and Central America and parts of 33 northern South America west of the Andes, one distributed across the Amazonian Basin and 34 35 central South America, and one restricted to the Guiana Shield. **Discussion.** The question as to whether these paranasal morphotypes may represent previously 36 37 unrecognized species is to be evaluated through a thorough revision of the *Dasypus* species 38 complex integrating molecular and morphological data. Remarkably, our recognition of a distinct morphotype in the Guiana Shield area is congruent with the recent discovery of a divergent 39 40 mitogenomic lineage in French Guiana. The inflation of the second medialmost pair of caudal 41 frontal sinuses constitutes an unexpected morphological diagnostic feature for this potentially 42 distinct species. Our results demonstrate the benefits of studying overlooked internal 43 morphological structures in supposedly cryptic species revealed by molecular data. It also



14	illustrates the under-exploited potential of the highly variable paranasal sinuses of armadillos for
15	systematic studies.

### Introduction

Detection of cryptic diversity and pertinent delimitation of extant taxonomic entities constitute a major challenge of current-day biological research as it may have critical implications on biodiversity conservation policies (Carstens et al., 2013). Cryptic species can be defined as "two or more species that are, or have been, classified as a single nominal species because they are at least superficially morphologically indistinguishable" (Bickford et al., 2007). According to this definition, the absence of diagnostic morphological character may have impeded the recognition of species. Depending on the case, this absence might be real (*i.e.*, populations of two cryptic species do not differ significantly in their entire anatomy) or spurious (*i.e.*, morphological differences have been overlooked).

Advanced methods of microcomputed tomography (µ-CT-sean) now enable an unprecedented assessment of internal anatomical structures, which can help uncovering previously concealed morphological differences between taxa. The development of these non-destructive methods permits internal anatomy to be easily and systematically investigated in many taxa. These methodological improvements offer great opportunities for morphology-based phylogenetic research. For animals such as mammals, internal structures like those of the skull certainly present a great wealth of anatomical features to be scrutinized (possibly as many as the external surface of the skull) for taxonomic and phylogenetic purposes (e.g., Farke, 2010; Macrini, 2012; Ruf, 2014; Billet, Hautier & Lebrun, 2015). There is therefore a possibility that



68

69

70

71

72

73

74

75

76

77

78

79

80

81

82

83

84

85

86

87

88

89

this large proportion of previously poorly explored morphological data contains undetected morphological differences between alleged cryptic taxa.

The pan-American nine-banded armadillo (Dasypus novemcinctus) presents the largest distribution of any living xenarthran species (McDonough and Loughry 2013), and constitutes an interesting model for Neotropical phylogeography. Several subspecies (five to seven) have been recognized within this species but their delineation and recognition are not consensual (Cabrera, 1958; McBee and Baker, 1982; Wetzel et al., 2008; McDonough & Loughry 2013). In fact, most potential diagnostic characters for these subspecific distinctions are seldom detailed, often inconstant, or based on a limited number of observations (e.g., Peters, 1864; Allen, 1911; Lönnberg, 1913; Hamlett, 1939; Hooper, 1947; Russell, 1953). Taxonomy and phylogeny in long-nosed armadillos (Dasypodidae, sensu Gibb et al., 2016) particularly suffer from strong disagreement between morphological and molecular data (Castro et al., 2015; Gibb et al., 2016). Even though it was more focused on higher taxonomic levels, a recent study suggested the existence of an unrecognized species in French Guiana based on mitochondrial data (incl. mitogenomes) (Gibb et al., 2016). The Guianan entity has never been distinguished from other D. novemcinctus on morphological bases, and might thus represent another striking case of cryptic species. In order to explore if internal parts of the skull contain a useful phylogenetic signal, we investigated the internal paranasal sinuses and recesses (Rossie, 2006), whose complex structure has largely been ignored by morphologists working on the systematics of long-nosed armadillos

has largely been ignored by morphologists working on the systematics of long-nosed armadillo (genus *Dasypus*). Based on images issued from microcomputed tomography of skulls, we reconstructed virtually the entire network of paranasal spaces in *Dasypus* species with a particular focus on specimens of *D. novemcinctus* covering the entire geographic range of the



species. The observed patterns are described and discussed considering traditional taxonomic entities of long-nosed armadillos and in light of most recent molecular findings. A focus is made on the discriminatory power of these concealed characters in armadillos and on their utility for diagnosing taxonomic units previously regarded as cryptic.

The total number of investigated specimens is composed of 136 skulls of *Dasypus* spp. harvested

94

90

91

92

93

95

96

97

98

110

111

112

### **Materials & Methods**

### Specimens and CT-scanning

from various institutions worldwide (see details in Table S1), among which 112 were identified 99 100 as D. novemcinctus, 1 as D. sabanicola, 13 as D. kappleri, 4 as D. hybridus, 3 as D. septemcinctus, and 3 as D. pilosus. Among this sample, we reconstructed virtually the internal 101 paranasal spaces in 51 CT-scanned specimens belonging to D. novemcinctus (n=47), D. kappleri 102 (n=1), D. hybridus (n=1), D. septemcinctus (n=1), and D. pilosus (n=1). Among the 47 D. 103 novemcinctus specimens, 7 were considered juveniles, including a potential stillborn (USNM 104 020920); the 40 remaining being adults or subadults. The 47 D. novemcinctus specimens came 105 from: United States (n=3), Mexico (n=4), Guatemala (n=1), Nicaragua (n=1), Costa Rica (n=1), 106 Panama (n=1), Colombia (n=6), Venezuela (n=2), Ecuador (n=2), Peru (n=2), Bolivia (n=2), 107 Paraguay (n=1), Guyana (n=3), Suriname (n=2), French Guiana (n=3), Brazil (n=12; see a list of 108 different states in Table S1), and Uruguay (n=1). Digital data of all 51 specimens were acquired 109

using X-ray micro-computed tomography ( $\mu$ CT). Most specimens were scanned on the X-ray

tomography imagery platform at the Université de Montpellier (France) and on the CT-scan

platform of the Imaging and Analysis Centre of the British Museum of Natural History (London,







UK); one (MNHN.ZM-MO 2001.1317) was scanned at the Museum National d'Histoire
Naturelle (France) in Paris (AST-RX platform). Detailed information about the scans and
acquisition parameters can be found in Table S1. Three-dimensional reconstructions and
visualizations of the frontal sinuses were performed using stacks of digital $\mu\text{CT}$ images with
AVIZO v. 6.1.1 software (Visualization Sciences Group 2009).
An additional subset of 65 D. novemcinctus, 1 D. sabanicola, 12 D. kappleri, 3 D.
hybridus, 2 D. septemcinctus and 2 D. pilosus specimens was added to the sample mentioned
above. These additional specimens correspond to i) skulls that allowed observing frontal sinuses
boundaries through bone transparency throughout direct observations or photographs (NB: this
was not possible for all observed skulls, some being insufficiently prepared or having no
transparency of the frontal bone) and/or to ii) CT-scanned skulls whose paranasal cavities were
not virtually reconstructed but their boundaries observed with ISE-Meshtools (Lebrun, 2008)
not virtually reconstructed but their boundaries observed with ISE-Meshtools (Lebrun, 2008) with an artificial cutting of the specimen following a coronal section and with the software
with an artificial cutting of the specimen following a coronal section and with the software
with an artificial cutting of the specimen following a coronal section and with the software  Landmark 3.6 (available at <a href="http://graphics.idav.ucdavis.edu/research/EvoMorph">http://graphics.idav.ucdavis.edu/research/EvoMorph</a> ; Institute for
with an artificial cutting of the specimen following a coronal section and with the software  Landmark 3.6 (available at <a href="http://graphics.idav.ucdavis.edu/research/EvoMorph">http://graphics.idav.ucdavis.edu/research/EvoMorph</a> ; Institute for  Data Analysis and Visualisation ©) with the option transparent surface rendering. These methods
with an artificial cutting of the specimen following a coronal section and with the software  Landmark 3.6 (available at <a href="http://graphics.idav.ucdavis.edu/research/EvoMorph">http://graphics.idav.ucdavis.edu/research/EvoMorph</a> ; Institute for  Data Analysis and Visualisation ©) with the option transparent surface rendering. These methods helped us to increase the number of investigated specimens and, most particularly, to include a
with an artificial cutting of the specimen following a coronal section and with the software  Landmark 3.6 (available at <a href="http://graphics.idav.ucdavis.edu/research/EvoMorph">http://graphics.idav.ucdavis.edu/research/EvoMorph</a> ; Institute for  Data Analysis and Visualisation ©) with the option transparent surface rendering. These methods helped us to increase the number of investigated specimens and, most particularly, to include a
with an artificial cutting of the specimen following a coronal section and with the software  Landmark 3.6 (available at <a href="http://graphics.idav.ucdavis.edu/research/EvoMorph">http://graphics.idav.ucdavis.edu/research/EvoMorph</a> ; Institute for  Data Analysis and Visualisation ©) with the option transparent surface rendering. These methods helped us to increase the number of investigated specimens and, most particularly, to include a
with an artificial cutting of the specimen following a coronal section and with the software  Landmark 3.6 (available at <a href="http://graphics.idav.ucdavis.edu/research/EvoMorph">http://graphics.idav.ucdavis.edu/research/EvoMorph</a> ; Institute for  Data Analysis and Visualisation ©) with the option transparent surface rendering. These methods helped us to increase the number of investigated specimens and, most particularly, to include a paratype specimen of <i>D. sabanicora</i> (Mondolfi, 1968) (Table S1).
with an artificial cutting of the specimen following a coronal section and with the software  Landmark 3.6 (available at <a href="http://graphics.idav.ucdavis.edu/research/EvoMorph">http://graphics.idav.ucdavis.edu/research/EvoMorph</a> ; Institute for  Data Analysis and Visualisation ©) with the option transparent surface rendering. These methods helped us to increase the number of investigated specimens and, most particularly, to include a paratype specimen of <i>D. sabanicora</i> (Mondolfi, 1968) (Table S1).  Nomenclature of paranasal anatomy



extensive work on paranasal spaces in Cingulata concerns in fact some glyptodonts (Fernicola et 136 al., 2012), whose sinuses are very different from that of long-nosed armadillos. For these 137 reasons, our nomenclature follows several conventions used in other taxa, as detailed below. The 138 standard practice for paranasal sinuses is to name them after the bones they excavate (Novacek, 139 1993); we respected this practice for all the cavities we detected (i.e., both sinuses and recesses). 140 141 The identity of the bones housing these cavities was determined through the examination of juvenile specimens that display clearly visible bone sutures. Following recent works by Maier 142 (2000), Rossie (2006), and Farke (2010), we made a distinction between sinus and recess for 143 paranasal cavities. Paranasal sinuses are pneumatic and mucosa-lined spaces that are located in 144 the bones surrounding the nasal chamber (Curtis & Van Valkenburg, 2014). Contrary to sinuses 145 that are found between two layers of cortical bones (e.g., frontal), paranasal recesses are defined 146 as simple concavities of the nasal cavity, and are not associated with active bone removal (Farke, 147 2010; Rossie, 2006). Hereafter, we employed the terms sinus or recess accordingly. Because 148 there are often several sinuses or recesses within a given bone (e.g., frontal, maxillary), we also 149 used the English equivalents of positional terms of the Nomina Anatomica Veterinaria (NAV, 150 2005) for the paranasal sinuses when feasible (e.g., caudal frontal sinus). It was not possible to 151 152 elaborate robust homology hypotheses for all cavities of the paranasal region because they are found in large numbers and may represent neoformations when compared to the common 153 154 terminology. Consequently, we complemented the common terminology with a numbering 155 system that allows distinguishing the numerous frontal recesses and sinuses found in long-nosed armadillos. The terminology for turbinal bones, which are only briefly mentioned for spatial 156 157 localization of paranasal cavities, is based on Van Valkenburgh, Smith & Craven (2014) and 158 Maier & Ruf (2014).





159	
160	Institutional abbreviations: AMNH, American Museum of Natural History, New York, USA;
161	BMNH, British Museum of Natural History (Natural History Museum), London, UK; IEPA
162	Instituto de Pesquisas Científicas e Tecnológicas do Estado do Amapá in Macapá, Brazil;
163	KWATA, Kwata Association collection, Cayenne, French Guiana; LSU, Louisiana State
164	University, Baton Rouge, LA, USA; MBUCV Museo de biología de la Universidad central de
165	Venezuela; MHNG, Muséum d'Histoire Naturelle in Geneva, Switzerland; MNHN.ZM.MO,
166	collections "Zoologie et Anatomie comparée, Mammifères et Oiseaux" of Muséum National
167	d'Histoire Naturelle, Paris, France; MUSM Museo de Historia Natural-Universidad Nacional
168	Mayor de San Marcos, Lima, Peru; RMNH, Naturalis Biodiversity Center, Leiden, Netherlands
169	(Rijksmuseum van Natuurlijke Historie); ROM, the Royal Ontario Museum in Toronto, Canada;
170	USNM, National Museum of Natural History, Smithsonian Institution; Washington, DC, USA.
171	
172	Anatomical abbreviations and measurements: CFS, caudal trontal sinus (numbered from 0 to 5);
173	FR, frontal bone; LA, lacrimal bone; LTC, length total cranium, measured from the anterior
174	nasal tip to the posteriormost extent of the nuchal occipital crests; NA, nasal bone; RFR, rostral
175	frontal recess (numbered from 1 to 3); RL, lacrimal recess (numbered from 1 to 2); RMXC,
<b>176</b>	caudal maxillary recess; RMXR, rostral maxillary recess.
177	
178	
179	Results
180	Observations common to all long-nosed armadillos (genus Dasypus)



In all investigated long-nosed armadillos, paranasal sinuses and recesses consistently excavate the same three bones of the cranial face and vault: the lacrimal, the maxillary and the frontal. Sinuses are present only in the frontal bone of *D. novemcinctus*, *D. pilosus*, and *D. kappleri*; they are absent or weakly marked in *D. hybridus* and *D. septemcinctus* (Fig. 1). Only the posterior pneumatic parts of the frontal bone form sinuses whereas, more anteriorly, the pneumatization of the frontal bone forms recesses, which are in direct contact with the underlying turbinals all along their anteroposterior length. In most adult individuals of *D. novemcinctus* (see more details below) and *D. kappleri*, the frontal sinuses almost entirely cover the posterior part of the fronto-and ethmoturbinals dorsally. In all species, the frontal sinuses and recesses regularly thicken dorsoventrally toward the front. The number of sinuses and recesses varies intragenerically and these structures will be described hereafter.

In all *Dasypus* species, recesses excavate the paranasal cavity dorsally and laterally. These recesses represent large free-of-bone spaces in the nasal cavity, generally separating turbinal bones medioventrally from the bones that build up the cranial walls. The lacrimal recesses are in contact with the mass of fronto- and ethmoturbinals medially, whereas the maxillary recesses cover the naso- and maxilloturbinals dorsolaterally. Two distinct lacrimal recesses are invariably present and are separated by the bony cover of the nasolacrimal duct. Two recesses, variably individualized, excavate the maxillary bone (Fig. 1) and are bordered by the nasolacrimal duct ventrolaterally.

In addition to the taxonomic and geographic variation described below, variable levels of intra-individual asymmetry appear to affect all species and all paired paranasal spaces under consideration here. This asymmetry is not directional, it is ubiquitous and present in most if not all specimens, which suggests a case of fluctuating asymmetry (Van Valen, 1962). The species



D. kappleri seems to be characterized by stronger levels of asymmetry than the species D.novemcinctus (see below).

### Juveniles of D. novemcinctus

In addition to delivering critical information on the identity of bones housing the various sinuses and recesses, the study of juvenile individuals provided some clues on the growth pattern of the paranasal pneumatization in the nine-banded armadillo. Juveniles show a less tight medial contact between paired medial sinuses, such as the rostral and intermediate frontal recesses (RFR1 and RFRT) or the caudal frontal sinuses 0 or 1 (Fig. 2). Compared to adults, caudal frontal sinuses (CFS) are less expanded posteriorly in juveniles and do not cover the most posterior part of the mass of fronto- and ethmoturbinals.

A very young specimen (likely a stillborn, AMNH 33150) shows that very early ontogenetic phases of paranasal pneumatization start with a weak individualisation of the caudal maxillary recess, whereas no other sinus or recess is individualized and the turbinals are not yet ossified. The large cavity excavated in the posterior part of the frontals in this specimen posteriorly does not represent a sinus but a transverse canal, presumably for the frontal diploic vein (Wible and Gaudin, 2004) (Fig. 3). Other juveniles in our dataset clearly correspond to later ontogenetic stages, as indicated by their size: LTC= AMNH33150 38,93mm; LSU3244 66,14mm; USNM020920 72,89mm; AMNH133259 68,85mm (NB: LTC ~ 90-105mm in adults; Hautier L., unpublished data). This age difference is confirmed by their stage of dental eruption: first decidual bicuspid tooth erupting in AMNH 33150; dP1-dP7 present in LSU3244 and USNM 20920; dP1-dP7 and alveolus of M1 present in AMNH 133259 (see Ciancio et al., 2011). The juvenile series shows that paranasal pneumatization and turbinal ossification just barely started in



227	perinatal stages lesser than 40% adult skull length (AMNH 33150; Fig. 3) whereas these
228	structures are well-developed in later stages with dp1-dp7 erupted and with $\sim 70\%$ of adult skull
229	length (Fig. 2).
230	
231	Observations common to all adults of nine-banded armadillos (D. novemcinctus)
232	Skulls of adult <i>D. novemcinctus</i> are more pneumatized than juvenile ones (Figs. 2-4). All adult
233	D. novemcinctus present a similar pattern of sinuses: posteriorly, a number of 5 to 6 paired CFS
234	generally cover dorsally the posterior part of the mass of fronto- and ethmoturbinals (Figs. 1, 4
235	and 5). These sinuses form a continuous transversal chain of dorsal paranasal spaces between the
236	orbits (Fig. 5). Anterior to these sinuses, the frontal bone houses several pairs of rostral frontal
237	recesses (RFR). These recesses show variable shapes (see below), but can be at least divided in
238	two main areas: a medial recess generally elongated (RFR1) and/or subdivided anteroposteriorly
239	(RFR1 & RFR1'), and a recess or group of recesses that excavate the frontal bone more laterally
240	up to the lacrimal recesses (RFR2-3) (Fig. 1). The CFS 0-1 are always located directly posterior
241	to the RFR1 and the CFS2-4 are located posterior to the RFR2-3.
242	
243	Northern morphotype of D. novemcinctus
244	Thirty nine (39) specimens from North and Central America and from the Pacific coast of
245	eastern Ecuador are attributed to this morphotype (Figs. 1 and 4). Specimens attributed to this
246	group originate from (in alphabetical order of countries): Belize, Colombia (Antioquia
247	Department), Costa Rica, Ecuador (Provinces El Oro and Pichincha), Guatemala, Honduras,
248	Mexico (Sinaloa, Tabasco, Oaxaca, Colima, Jalisco, and an undetermined state (USNM 179172)
249	for the adults, San Luis Potosi and Morelos for the juveniles), Nicaragua, and USA (states of



250	Mississipi, Texas, Florida, Kansas, and Louisiana). The main diagnostic feature for this group is
251	the anteroposterior elongation of the CFS2 to 5; in addition, the left and right CFS2 are obliquely
252	orientated and contact each other posterior to the CFS1. Another distinctive feature of this
253	morphotype is the subdivision and the relative shortening of RFR1. As for the Southern
254	morphotype (see below), the number of CFS pairs in this group varies from 5 to 6, because the
255	CFS0 pair is either very reduced or absent. The medialmost CFS have been numbered to because
<b>256</b>	of their variable presence; on the contrary, CFS1-5 are always present. The CFS1 are rather
257	small, shorter than the more lateral CFSs and bordered posteriorly by the contacting pair of
258	CFS2. The CFS2 and/or CFS3 are the largest CFSs within this group, and though they do not
259	contact posteromedially, each CFS3, similarly to the CFS2, bends or orientates obliquely toward
260	the midline posteriorly. The CFS4 can be as elongated as the CFS2-3 or slightly smaller; the
261	CFS5 are more reduced. The median rostral frontal recesses are subdivided into two
262	anteroposterior pairs RFR1 and RFR1' and contrast with the long RFR1 of the Southern
263	morphotype. The posterior pair, the RFR1, apparently forms earlier within the ontogenetic
264	sequence as it is clearly more developed than RFR1' in two juvenile specimens from Mexico
265	(Fig. 2). The shape of RFR1 in adults is rather square whereas the anterior pair, RFR1', is
266	usually slightly more elongated anteroposteriorly. Lateral to the RFR1 and RFR1', the RFR2 and
267	3 are often well separated (distinction often better marked than in the Southern group); the RFR3
268	is immediately lateral to the RFR2. The same applies to the caudal and rostral maxillary recesses
269	(RMXC & RMXR), which are often better separated in this morphotype compared to the
270	Southern morphotype; the caudal maxillary recess is posterolateral to the rostral one and located
271	just anterior to the lacrimal recess 2.



The specimen AMNH 40984 from southwest Ecuador is attributed to this Northern group because of the presence of large and posteriorly convergent CFS2 and short and subdivided RFR1-RFR1' (Fig. 4). The other specimen from western Ecuador, BMNH 16.7.12.37, also shows these characters through bone transparency. Nevertheless, on the virtual reconstruction of AMNH 40984, the lateral RFR2-3 appear more subdivided than in other members of this morphotype, and also more than in other morphotypes. In addition, the anterior edge of its medialmost CFS (CFS 0) is shifted anteriorly. These unique characters could not be checked on the specimen observed on photos only.

### Southern morphotype of D. novemcinctus

Fifty one (51) specimens (incl. the paratype of *D. sabanicola*) spanning the Amazon Basin (excluding the Guiana Shield) and including the southernmost distribution of the species in Uruguay show a distinct pattern of paranasal spaces (Fig. 4). Specimens attributed to this group thus span the Southern range of *D. novemcinctus* and originate from the following countries (in alphabetical order): Bolivia (states of Beni, Pando and Santa Cruz), Brazil (states of Amazonas, Para, Goias, Santa Catarina, Mato Grosso, Mato Grosso do Sul, Minas Gerais, São Paulo, Rio Grande do Sul and Espirito Santo), Colombia (Meta and Magdalena departments), Ecuador (Morona Santiago Province), Paraguay, Peru (regions of Ucayali, Ayacucho and San Martín), Uruguay, and Venezuela (states of Anzoátegui and Apure (state of the paratype of *D. sabanicola*)). The distinctive features of the Southern pattern of paranasal spaces mostly consist in an anteroposteriorly reduced posterior chain of caudal frontal sinuses and an elongated rostral frontal recess 1 (Figs. 1 and 4). In this group, the CFS0 are variably present. When present, they are generally smaller than the more lateral CFS1 to 5. The CFS1 always contact each other



medially, or just at their posteromedial corner if the CFS0 are present. In most specimens, the CFS are much shorter anteroposteriorly than the rostral frontal recess RFR1, usually around a 1/2 or 1/3 ratio. Some specimens referred to this morphotype show more balanced ratios but the anteroposterior length of the CFS never exceeds that of the RFR1. The CFS1 to 4 are usually of similar length and width, the areas of the CFS 1 and 2 may just slightly exceed that of the others in average. The lateralmost caudal frontal sinus that lies immediately medial to the orbital rim, i.e. the CFS5, is generally shorter than the other CFS.

Additionally, many individuals of that group show a weak distinction or even a fusion between the RFR2 and 3 (Figs. 1 and 4). Though the RFR2 and 3 are in average less separated than in other groups of *D. novemcinctus*, this character is not stable within the Southern group. Ontogenetic data are unfortunately lacking to state on a possible influence of development on this feature. When not completely fused, the RFR 2 and 3 are often separated by a short bony ridge posteriorly.

The maxillary recesses are located dorsal to the nasolacrimal duct and (antero)lateral to the RFR1. As for the RFR2 and 3, the caudal and rostral maxillary recesses are variably distinct; in average, they are less separated than in the other groups.

#### Guianan morphotype of D. novemcinctus

Seventeen (17) specimens are attributed to this group and originate from: Brazil (Amapa State), French Guiana, Guyana and Suriname. The most conspicuous diagnostic feature of this group is the strong inflation of the CFS2, which is by far the largest caudal frontal sinus (Figs. 1, 4 and 5). These hypertrophied CFS2 occupy most or all the pneumatized frontal area between the orbits up to the level of the anterior edge of the posterior zygomatic root posteriorly. More precisely, it is



the posterior part of the CFS2 that is hypertrophied and borders all or most other CFSs on their caudal side. The anterior part of the CFS2, which is sandwiched between CFS1 and CF3, is as narrow as the CFS3-4. The outline of CFS2 often exhibits a complex irregular pattern and pairs are clearly asymmetric in all specimens (Fig. 4).

The CFS0 are variably present as in other groups. When present, they are rather small, clearly elongated transversally and entirely bordered by the CFS1 posteriorly. In comparison to other morphotypes, the CFS0 are slightly shifted anteriorly relative to other CFSs. The size and shape of the CFS1 is also variable. In specimens with no CFS0, the CFS1 are much reduced and rather square-shaped (AP 207; Fig. 4). In specimens with CFS0, the CFS1 are relatively larger and can extend as far posteriorly as the hypertrophied CFS2. In such case (MNHN.ZM-MO 2001-1317), they are transversally thin and sandwiched between the pairs of CFS2 (Fig. 4). In one specimen (MNHN.ZM-MO 1996-587), the CFS1 seems to be partly fused posteromedially with the CFS2 on both sides. The CFS3 and 4 are considerably smaller than the CFS2, and are similar in size as in the Southern morphotype. The CFS5 is generally smaller than CFS3-4, and can be absent (*e.g.*, MNHN.ZM-MO 2001-1317).

The configuration of the RFR1 is variable, as they seem to be irregularly divided into an anterior RFR1' and posterior RFR1. The limits between these two subdivisions are not only variable between individuals of this morphotype, they are also labile intra-individually: the subdivisions may be marked on one side of the skull, not on the other (ROM 32275) or it may follow another path (MNHN.ZM-MO 1995-553), or the boundaries may be irregularly marked overall (marked on some portion, then absent, and then marked again a little farther away; USNM 339668). As in the Southern morphotype, the RFR2 and 3 are poorly distinguishable in





340	most Guianan specimens (but this is also variable), except for a posterior demarcation that is
341	almost always present.
342	The lacrimal recesses 1 and 2 are very similar to that of the other morphotypes, also
343	delimited by the nasolacrimal duct. The intensity of the separation between the rostral and caudal
344	maxillary recesses is variable, but these recesses are otherwise very similar to other
345	morphotypes.
346	
347	Problematic Specimens from Panama, Venezuela and Colombia
348	Five specimens (AMNH 32356, 37356, USNM 281290 from Colombia, BMNH 5-7-521 from
349	Merida, Venezuela and USNM 171052 from Panama) show somewhat intermediate
350	morphologies between the Southern and Northern morphotypes (Fig. 4). They all present CFS
351	and RFR1 of similar length and do not show a medially contacting pair of CFS2 (though close in
352	AMNH 37356). The RFR1 are usually not subdivided, except in the Venezuelan specimen and,
353	to a lesser extent, in the Colombian AMNH 32356. The CFS2 and 3 do not represent the largest
354	CFS except in the Colombian AMNH 32356 and 37356. These specimens therefore show a
355	combination of features characterizing the Southern and Northern groups.
356	In addition, the probable stillborn specimen AMNH 33150 from Colombia could not be referred
357	to any morphotype because its paranasal spaces are not individualized (rig. 3).
358	
359	Other Dasypus Species
360	Greater long-nosed armadillo (D. kappleri)
361	The $D$ . $kappleri$ specimens present a large pneumatization of their paranasal region, as in $D$ .
362	novemcinctus. However, all D. kappleri specimens exhibit less numerous, but wider and longer



finger-shaped CFS than *D. novemcinctus*. In fact, this may be due to various partial or complete fusions of the CFS with the RFR, which we tentatively identify as follows: the CFS1 and RFR1 are fused and occupy the medialmost region (but not posteriorly in some specimens; see below), the CFS2-3 are fused with the RFR2-3 (Fig. 1). On some specimens, a blunt bony bridge still marks a separation between these sinuses and recesses. This general pattern is typical of the species, yet the arrangement of paranasal cavities largely varies intraspecifically. Two groups can be distinguished: specimens from the Guiana Shield display fused CFS1-RFR1 that reach the posterior boundary of the other CFS, whereas specimens from more western locations have the right and left CFS2 that contact posteriorly in the midline (Fig. S2). The relative sizes of the CFS also vary a lot, but the fused CFS2-3 with RFR2-3 are in most cases the largest ones. In addition, most of these recesses show a substantial amount of asymmetry, probably higher than in *D. novemcinctus*. Other recesses are grossly similar in size and location to those described for *D. novemcinctus*.

Hairy long-nosed armadillo (D. pilosus)

The investigated specimens of *D. pilosus* probably resemble the most to-the *D. novemcinctus* groups (Fig. 1). Conversely to *D. kappleri*, specimens of *D. pilosus* show caudal frontal sinuses well-individualized from the rostral frontal recesses. However, there is some variation in the shape of the caudal frontal sinuses. In the only scanned specimen of *D. pilosus*, the caudal frontal spaces are barely recognizable as they do not excavate the frontal bone (not found between two layers of frontal bone); they are located just dorsal to the mass of fronto- and ethmoturbinals. In fact, they rather represent thin cell-shaped recesses with irregular outlines, which are sandwiched between the frontal bone dorsally and the fronto- and ethmoturbinals ventrally. Conversely, the





387

388

389

390

391

392

393

394

395

396

397

398

399

400

401

402

403

404

405

406



two additional specimens of *D. pilosus* observed through bone transparency show slightly longer caudal frontal sinuses that are better delineated. In any case, the caudal cell-shaped frontal sinuses are in all three specimens comparable to the CFS of D. novemcinctus groups in their number (4 to 5 pairs), dorsal outline and location. The rather short anteroposterior extent and reduced mediolateral width of the CFS of D. pilosus are most reminiscent of the pattern seen in the Southern group of D. novemcinctus. The more anterior recesses resemble the RFR1 and RFR2-3 of the same Southern group, especially the un(sub)divided and elongated RFR1. Remarkably, the lacrimal recesses are more elongated anteroposteriorly than in other *Dasypus* species. Southern long-nosed armadillo (D. hybridus) and seven banded armadillo (D. septemcinctus) These two species are here described together because they exhibit strong similarities in their pattern of paranasal cavities and could not be distinguished in our sample. These two small-sized species show the least pneumatized skulls among of our adult sample of *Dasypus*. Both species present RFR1 that are transversely narrow and curved, never in contact medially, and thus partly recall the configuration seen in young D. novemcinctus specimens (see above) (Figs. 1-2). In addition, specimens of both species have poorly defined CFS, i.e., the fronto- and ethmoturbinals fill in most of the space just ventral to the cranial vault made by the frontals and the CFS are very thin dorsoventrally. The frontal bones are in fact poorly pneumatized and show

a thin diploe. Other cavities (rostral frontal recesses, lacrimal and maxillary recesses) show a

pattern and extent grossly similar to that of other *Dasypus* species.

407

408

### **Discussion**



Distribution and significance of paranasai pneumatization in mammais and armaatios
Paulli (1900a; 1900b) first provided detailed descriptions of paranasal cavities based on sagittal
and transverse osteological sections of mammalian skulls. With the recent development of
micro-tomography and virtual modeling of internal structures, the paranasal sinuses and recesses
could be more systematically and precisely studied in extant mammals such as vombatiform
marsupials, carnivorans, artiodactyls and primates (e.g., Rossie, 2008; Farke, 2010; Curtis & Van
Valkenburg, 2014; Maier & Ruf, 2014; Sharp, 2016). Though not yet thoroughly investigated
with modern techniques, these structures are also known to occur in many other groups of
placental mammals (Paulli, 1900a; Paulli, 1900b; Edinger, 1950; Novacek 1993) and may
constitute convergently lost symplesiomorphic placental features (Foster & Shapiro, 2016).
The ubiquitous distribution of these structures in several clades of amniotes (Witmer,
1999) long raised questions regarding the potential functional role of paranasal pneumatization.
As noted by Farke (2010: 988), cranial pneumatization such as paranasal sinuses "remains one of
the most functionally enigmatic and debated structures within the vertebrate skull". Indeed,
researchers have long speculated on the potential functional role of these air-filled chambers, and
proposed a wealth of hypotheses (Blanton & Biggs, 1969; Blaney, 1990; Marquez, 2008), most
of which remain, as of today, untested. However, one of the current dominating hypotheses
regards sinuses as functionless structures influenced by constraints inherent to bone growth and
patterning (Farke, 2010 and citations therein). In fact, sinuses may just opportunistically fill
space where bone is not mechanically necessary (Curtis & Van Valkenburg, 2014) and reduce
skull mass in return (Curtis et al., 2015). This might be compatible with the fact that the presence
and extent of sinuses may, at least in some instances, be linked to size increase and to the shape
of the bone in which they are contained (Weidenreich, 1941; Zollikofer et al., 2008; Farke, 2010;



alternative architectural explanations do not preclude the existence of functional advantages 433 (e.g., to dissipate stress: Tanner et al., 2008), it seems that there is no overarching explanation for 434 the function of sinuses (Curtis et al., 2015). 435 A substantial variation of paranasal sinuses shape and outline has long been noted in 436 437 many taxa at the interspecific, intraspecific, and intra-individual levels (e.g., Paulli, 1900a; Paulli, 1900b; Novacek, 1993; Farke, 2010; Curtis & Van Valkenburg, 2014). These 438 observations clearly suggest that these structures have a non-negligible propensity to vary greatly 439 in mammals. It is questionable whether or not their high variability (sensu Hallgrímsson & Hall, 440 2005) could make paranasal sinuses good markers of phylogenetic history. Interestingly, the 441 highly variable shape and size of the frontal sinus in modern humans proved to be largely 442 inherited from parents to children (Szilvássy, 1982) and is used in forensic science for individual 443 and population identifications (e.g., Kim et al., 2013). At higher taxonomic levels, a significant 444 phylogenetic signal was detected in the pattern of paranasal sinuses of primates and bovid 445 artiodactyls (Rossie, 2008; Farke, 2010), but the size and shape frontal sinuses were not tightly 446 linked with phylogenetic groupings in Carnivora (Curtis & Van Valkenburg, 2014). Similarly, 447 448 the diversity of maxillary sinuses in macaques was not linked to phylogeny (Ito & Nishimura 2016) even though these structures were at least in part controlled by intrinsic genetic factors (Ito 449 et al., 2015). 450 451 In the case of long-nosed armadillos, the clear discrete differences in patterns of paranasal sinuses observed between the different species and subgroups of *Dasypus (D. novemcinctus, D.* 452 453 kappleri, D. pilosus, D. septemcinctus and D. hybridus) argue for a high discriminatory power 454 and a good phylogenetic signal carried by these structures within the genus. The fluctuating

Curtis et al., 2015; Krentzel & Angielczyk, 2016; Ito & Nishimura, 2016). Though these



456

457

458

459

460

461

462

463

464

465

466

467

468

469

470

471

472

473

474

475

476

477

asymmetry (Van Valen, 1962) tentatively identified for these structures in armadillos suggests that they are also impacted by random perturbations of developmental processes (Klingenberg, 2010). Curiously, early anatomical accounts of paranasal anatomy disagreed on the presence of sinuses in long-nosed armadillos. While Cuvier (1845) and Weinert (1925) correctly observed the presence of such structures in long-nosed armadillos, other early authors overlooked it (Paulli, 1900b; Zuckerkandl, 1887 (as cited in Weinert, 1925)). In fact, frontal sinuses were still considered absent in armadillos as a whole in recent anatomical works (Novacek, 1993). Our results clearly contradict these considerations and investigation of paranasal cavities in some Chlamyphoridae, the sister group of Dasypodidae within Cingulata (Gibb et al., 2016), even reveals homoplastic evolution of these structures in armadillos. Frontal sinus or recesses are absent in the extant chlamyphorid *Euphractus sexcinctus* (Wible & Gaudin, 2004) and some CTscanned specimens of Cabassous unicinctus (MNHN.ZM.MO 1953-457) and Zaedyus pichiy (MNHN.ZM.MO 1917-135) do not show any free-of-bone space between the frontal and the frontoethmo-turbinals (personal observations). On the other hand, an extensive system of paranasal sinuses exists in the extinct glyptodont *Neosclerocalyptus* (Fernicola et al., 2012). Further comparisons are needed in extant and fossil forms (see sinuses in the fossil *D. punctatus*, Castro et al., 2013), as these structures might provide potentially interesting characters for the understanding of higher-level relationships within the order (Delsuc et al., 2016). Relevance of paranasal sinuses for the systematics of long-nosed armadillos Our detailed investigation of paranasal cavities in *Dasypus* species revealed an important variation at different levels. We first described the ontogenetic pattern of the paranasal sinuses

and recesses, which probably start individualizing in perinatal stages. Postnatal juvenile



479

480

481

482

483

484

485

486

487

488

489

490

491

492

493

494

495

496

497

498

499

500

specimens show CFS that are less developed posteriorly when compared to adult specimens, revealing the late posterior growth of these structures. Second, as indicated above, adults show clear differences between traditionally recognized species, mostly in the configuration of the CFS and RFR. Besides the large variation seen within *D. novemcinctus* (see below), clear differences can be observed between D. kappleri, D. pilosus and the sister species D. hybridus -D. septemcinctus. The greater long-nosed armadillo (D. kappleri) probably has the most divergent morphology regarding these sinuses and recesses with the fusion of its CFS and RFR. In contrast, these structures are better separated in all other long-nosed armadillos reconstructed here. This is congruent with the early diverging position of D. kappleri in the phylogeny of longnosed armadillos (Gibb et al., 2016). Our sample for D. kappleri is also characterized by a substantial variation, which is partly structured geographically: specimens from the Guiana Shield show a CFS1-RFR1 that reaches the posterior level of other CFS, whereas this is not the case in other specimens originating from more western areas in South America (Fig. S2). Interestingly, these two allopatric groupings are congruent with the new taxonomic subdivision proposed by Feijo & Cordeiro-Estrela (2016), with a revised D. kappleri species restricted to the Guiana Shield area, and a new species (*D. pastasae*) found from the eastern Andes of Peru, Ecuador, Colombia, and Venezuela south of the Orinoco River into the western Brazilian Amazon Basin. These preliminary results now require a larger sample, including specimens referred to D. beniensis (Feijo & Cordeiro-Estrela, 2016), in order to further test species delimitation in the *D. kappleri* complex. The pattern of paranasal cavities of the hairy long-nosed armadillo (D. pilosus) is more similar to the Southern morphotype of D. novemcinctus than to any other morphotype, which may have important implications on the reconstruction of its phylogenetic affinities. Castro et al.



502

503

504

505

506

507

508

509

510

511

512

513

514

515

516

517

518

519

520

521

522

523

(2015) found this species to be the sister group of all other species attributed to the genus Dasypus, and therefore proposed to place it in its own genus Cryptophractus. This early diverging position and generic status is in disagreement with a more recent mitogenomic analysis, which retrieved D. pilosus in a more nested position within the genus Dasypus, with D. *kappleri* representing the earliest diverging species (Gibb et al., 2016). Remarkably, our findings may provide new morphological arguments for such a nested position of D. pilosus as unambiguously supported by molecular data. The related species D. septemcinctus and D. hybridus, for their part, closely resemble each other, as it could have been expected given their overall morphological resemblance and their phylogenetic proximity. This observation adds to the growing body of evidence that these two parapatric species might in fact represent a single taxonomic entity with a large distribution (Abba & Superina, 2010; Gibb et al., 2016). Most importantly, the variation within the nine-banded armadillo (Dasypus novemcinctus) allowed clearly separating three distinct geographical groups based on the pattern of paranasal cavities (Fig. 6). These individual subsets do not exactly correspond to traditional subspecies proposed for the nine-banded armadillo (McBee & Baker, 1982) though the distinction between the Northern and Central American (Northern morphotype) and the Southern American (Southern morphotype) groups may recall some subspecific boundaries (see below). In fact, although bone transparency often offers the possibility to observe the boundaries between the frontal sinuses and recesses, it seems that these characters have long been overlooked in cingulate systematics. The most interesting result lies in the distinction of a well-characterized entity restricted to the Guiana Shield area. Guianan nine-banded armadillos are distinguished by an inflated CFS2 in comparison to all other armadillos investigated here. The irregular outline of the CFS2 varies greatly among individuals belonging to the Guianan morphotype but its large



size relative to other CFS appears distinctive. While nine-banded armadillos from the Guiana
Shield have never been distinguished as a subspecies (i.e. they were until now considered as part
of the subspecies D. novemcinctus novemcintus Linnaeus 1758; Wetzel et al., 2008),
mitochondrial data showed that populations from French Guiana may represent an early
diverging and previously unrecognized lineage clearly separated from other D. novemcinctus
(Gibb et al., 2016; Arteaga M-C, unpublished data). Specimens from French Guiana present
unexpectedly distant mitochondrial D-loop region (Huchon et al., 1999) and divergent
mitogenomes (Gibb et al., 2016) from the invasive US populations of nine-banded armadillos.
Based on these new data, nine-banded armadillos from French Guiana are supposed to have
diverged 3.7 Ma ago from a clade formed by other D. novemcinctus, D. sabanicola, D. mazzai
and D. pilosus (Gibb et al., 2016). In this regard, the new data on paranasal cavities deliver
unprecedented and very enlightening results: there exists a discrete morphological signal of
internal cranial structures that supports the distinctness not only of French Guianan specimens,
but also of specimens from Suriname, Guyana and the state Amapa in Brazil (Fig. 6). Based on
this distribution, we refer to this entity as specimens from the Guiana Shield (or Guianan
specimens) whereas we do not know the exact outline and boundaries of the range occupied by
these distinctive armadillos. Taken together with recent mitogenomic data (Gibb et al., 2016) and
analyses of cranial shape variation (Hautier L., unpublished data), the paranasal autapomorphies
found in this study make a strong case for the distinction of nine-banded armadillo specimens
from the Guiana Shield as a potentially new species. The discovery of discrete paranasal
characters supporting this purportedly distinct species demonstrates the necessity to study
internal anatomy for a truly integrative taxonomy.



547

548

549

550

551

552

553

554

555

556

557

558

559

560

561

562

563

564

565

566

567

568

The number and delimitation of subspecies recognized within D. novemcinctus has long been a matter of debate among armadillo taxonomists (Cabrera, 1958; McBee & Baker, 1982; McBee, 1999; Wetzel et al., 2008; McDonough & Loughry 2013). Alongside the Guianan morphotype, the study of paranasal cavities also permitted to distinguish a mostly North and Central American morphotype (Northern group) and another South American morphotype (Southern group), which largely comes from the Amazon area (Fig. 6). The Northern morphotype is characterized by i) an anteroposterior elongation of the CFS2 to 5, with the obliquely oriented pair of CFS2 contacting each other posteromedially, and ii) subdivided and relatively shortened RFR1. The area where this morphotype is found fully covers the proposed repartition of the subspecies D. novemcinctus mexicanus (Peters, 1864), D. novemcinctus davisi Russel 1953, and part of D. novemcinctus fenestratus Peters 1864, and D. novemcinctus aequatorialis Lönnberg 1913 (McBee & Baker, 1982; Wetzel et al., 2008; McDonough & Loughry, 2013). It is generally well distinguished from the Southern morphotype, which is characterized by an anteroposteriorly reduced posterior chain of CFS and an elongated RFR1 (Fig. 6). The area occupied by specimens belonging to this morphotype corresponds mostly to the subspecies D. novemcinctus novemcintus (to the notable exception of the Guiana Shield area) and may also cover the distribution of D. novemcinctus mexianae Hagmann 1908 (Wetzel et al., 2008). Problematic specimens whose pattern of paranasal sinuses is not easily referable to one of the three main morphotypes are present in Panama and in the eastern parts of Colombia and Venezuela (Fig. 6). This geographic area also partly corresponds to the subspecies D. novemcinctus fenestratus (Wetzel et al., 2008). The partial incongruence of these internal data with recognized subspecies of D. novemcinctus raises important taxonomic issues. In addition,



these challenging results may also call into question the validity of the debated species *Dasypus sabanicola* (Mondolfi, 1968; Abba & Superina, 2010; Gibb et al., 2016), whose paratype MBUCV 439 exhibits the pattern of paranasal cavities of the *D. novemcinctus* Southern morphotype. However, this paratype represents a subadult specimen (Mondolfi, 1968), which casts doubts on the growth stage exhibited by its paranasal cavities (NB: other specimens attributed to this species could not be checked). The possibility also exists that this morphotype represents a plesiomorphic condition within the genus, since *D. pilosus* also exhibits a similar pattern. The question as to whether or not the three *D. novemcinctus* paranasal morphotypes represent natural taxonomic entities is now to be evaluated through a thorough revision of the *Dasypus* species complex that should integrate various morphological aspects and substantial molecular data (Hautier L., unpublished data; Arteaga M-C., unpublished data). The case of the problematic specimens found in Colombia, Venezuela and Panama clearly illustrates this necessity.

### **Conclusions**

As an early worker on *Dasypus* systematics, Hamlett (1939: 335) noted that in spite of the dispersion of *D. novemcinctus* through many geographical regions, "it remains so uniform that it is apparently impossible to find external variations sufficiently constant to be of subspecific rank". In fact, he suspected that cranial characters could offer the only promise for subspecific analysis of the species. These words resonate particularly, as the strong geographical imprint found in the variation pattern of paranasal cavities sheds new light on the delimitation of *D. novemcinctus* and its subspecies. As demonstrated in this work, the investigation of frontal sinuses may help to uncover previously overlooked phylogenetic subsets within the large



593

594

595

596

597

598

599

600

geographic range of nine-banded armadillos. This study highlights the under-exploited potential of internal characters for systematic studies and their utility for detecting otherwise potentially cryptic species. The strong variation and high discriminatory power found in the paranasal sinuses of armadillos is even strangely reminiscent of the extremely variable frontal sinuses of modern humans which can be used as forensic fingerprints (Kim et al., 2013) and kinship markers (Szilvássy, 1982; Slavec, 2005). In addition to its great potential for extant species, the study of the paranasal spaces also constitutes a promising approach to provide new informative characters for the phylogenetic placement of fossil species of the genus *Dasypus* (e.g., see partly exposed frontal sinuses in *D. punctatus*; Castro et al., 2013).

601

602

### Acknowledgements

We are grateful to Géraldine Véron and Aurélie Verguin (Muséum National d'Histoire Naturelle, 603 Paris), Roberto Portela Miguez, Louise Tomsett, Laura Balcells and Paula Jenkins (British 604 Museum of Natural History, London), François Catzeflis and Suzanne Jiquel (Institut des 605 Sciences de l'Evolution, Montpellier), Victor Pacheco (Dpto de Mastozoología, Museo de 606 Historia Natural, Universidad San Marcos, Lima), Eileen Westwig (American Museum of 607 Natural History, New-York), Burton Lim (Royal Ontario Museum, Toronto), Edmison Nicole 608 and Chris Helgen (National Museum of Natural History, Washington), Jake Esselstyn (Louisiana 609 State University, Bâton-Rouge), Manuel Ruedi (Muséumd'Histoire naturelle, Geneva), Claudia 610 Regina da Silva (Instituto de PesquisasCientíficas e Tecnológicas do Estado do Amapá, 611 Macapá), Steven van der Mije (Naturalis Biodiversity Center, Leiden), Lucile Dudoignon 612 613 (KWATA association), Maria-Clara Arteaga, Maria Nazareth da Silva (Manaus Museum) and their collaborators for access to comparative material. R. Lebrun (Institut des Sciences de 614



l'Evolution, Montpellier), Farah Ahmed (British Museum of Natural History, London), Miguel
García-Sanz (Platform AST-RX MNHN) generously provided help and advice on the acquisition
of CT scans. Thanks to Sandrine Ladevèze for providing CT-scan data for Cabassons and
Zaedyus. This is contribution ISEM 2017-XXX of the Institut des Sciences de l'Evolution.
Funding Statement
This work has benefited from an "Investissements d'Avenir' grant managed by Agence Nationale
de la Recherche, France (CEBA, ref. ANR-10-LABX-25-01). This research received support
from the Synthesys Project ( <a href="http://synthesys3.myspecies.info/">http://synthesys3.myspecies.info/</a> ), which is financed by the
European Community Research Infrastructure Action under the FP7.
Grant Disclosures
The following grant information was disclosed by the authors:
Agence Nationale de la Recherche: contract ANR-10-LABX-25-01.
Competing Interests
The authors declare no competing interests.
Author Contributions
• Guillaume Billet conceived and designed the experiments, contributed materials, performed the



638	experiments, analysed the data, wrote the paper.
639	• Lionel Hautier conceived and designed the experiments, contributed materials, performed the
640	experiments.
641	• Benoit de Thoisy contributed materials.
642	• Frédéric Delsuc conceived and designed the experiments, contributed materials.
643	• All authors read, discussed, corrected, and approved the final version of the paper.
644	
645	
646	References
647	Abba AM, Superina M. 2010. The 2009/2010 armadillo Red List assessment. <i>Edentata</i> 11:135–
648	184.
649	
650	Allen GM. 1911. Mammals of the West Indies. Bulletin of the Museum of Comparative Zoology
651	54:175-263.
652	
653	Bickford D, Lohman DJ, Sodhi NS, Ng PK, Meier R, Winker K, Ingram KK, Das I. 2007.
654	Cryptic species as a window on diversity and conservation. Trends in Ecology & Evolution 22
655	(3):148-155.
656	
657	Billet G, Hautier L, Lebrun R. 2015. Morphological diversity of the bony labyrinth (inner ear) in
658	extant xenarthrans and its relation to phylogeny. <i>Journal of Mammalogy</i> 96(4):658–672.
659	
660	Blaney SPA. 1990. Why paranasal sinuses? <i>Journal of Laryngology and Otology</i> 104:690–693.



201	
562	Blanton PL, Biggs NL. 1968. Eighteen hundred years of controversy: the paranasal sinuses.
563	American Journal of Anatomy 124:135–147.
564	
565	Cabrera A. 1958. Catalogo de los mamíferos de América del Sur. Revista del Museo Argentino
566	de Ciencias Naturales "Bernardino Rivadavia," Buenos Aires 4:1-307.
567	
568	Carstens BC, Pelletier TA, Reid NM, Satler JD. 2013. How to fail at species delimitation.
569	Molecular Ecology 22(17):4369-4383.
570	
571	Castro MC, Ciancio MR, Pacheco V, Salas-Gismondi RM, Bostelmann JE, Carlini AA. 2015.
572	Reassessment of the hairy long-nosed armadillo "Dasypus" pilosus (Xenarthra, Dasypodidae)
573	and revalidation of the genus Cryptophractus Fitzinger, 1856. Zootaxa 3947:30-48.
674	
675	Castro MC, Ribeiro AM, Ferigolo J, Langer MC. 2013. Redescription of Dasypus punctatus
576	Lund, 1840 and considerations on the genus <i>Propraopus</i> Ameghino, 1881 (Xenarthra,
677	Cingulata). Journal of Vertebrate Paleontology 33(2):434-447.
678	
579	Ciancio MR, Castro MC, Asher RJ. 2012. Evolutionary implications of dental eruption in
680	Dasypus (Xenarthra). Journal of Mammalian Evolution 19:1–8.
581	
582	Curtis A, Van Valkenburgh B. 2014. Beyond the sniffer: frontal sinuses in Carnivora. <i>The</i>
583	Anatomical Record 297:2047-2064.





84	
85	Curtis A, Lai G, Wei F, Van Valkenburgh B. 2015. Repeated Loss of Frontal Sinuses in Arctoid
86	Carnivorans. Journal of Morphology 276:22–32.
87	
888	Cuvier G. 1845. Leçons d'anatomie comparée de Georges Cuvier, recueillies et publiées par M.
89	Duméril, 2nde édition. Tome troisième contenant le système nerveux et les organes des sens.
90	Paris: Fortin, Masson et Cie. 760 pp.
91	
592	Delsuc F, Gibb GC, Kuch M, Billet G, Hautier L, Southon J, Rouillard J-M, Fernicola JC,
593	Vizcaino SF, MacPhee RDE, Poinar HN. 2016. The phylogenetic affinities of the extinct
94	glyptodonts. Current Biology 26:R141–R156.
595	
596	Edinger T. 1950. Frontal sinus evolution (particularly in the Equidae). Bulletin of the Museum of
597	Comparative Zoology at Harvard College 103:411–496.
598	
599	Farke AA. 2010. Evolution and functional morphology of the frontal sinuses in Bovidae
700	(Mammalia: Artiodactyla), and implications for the evolution of cranial pneumaticity. Zoologica
701	Journal of the Linnean Society 159:988–1014.
702	
703	Feijo A, Cordeiro-Estrela P. 2016. Taxonomic revision of the <i>Dasypus kappleri</i> complex, with
704	revalidations of Dasypus pastasae (Thomas, 1901) and Dasypus beniensis Lönnberg, 1942
705	(Cingulata, Dasypodidae). Zootaxa 4170(2):271–297.
706	



/0/	refinedia JC, Toledo N, Bargo S, Vizcamo S. 2012. A neomorphic ossification of the hasar
708	cartilages and the structure of paranasal sinus system of the glyptodont Neosclerocalyptus Paula
709	Couto 1957 (Mammalia, Xenarthra). Paleontologia Electronica 15(3):1-22.
710	
711	Foster FR, Shapiro DF. 2016. Convergent loss of paranasal sinuses in mammals is explained by
712	their deleterious effects on high-frequency communications. <i>The Anatomical Record</i> 299: 133.
713	
714	Gibb GC, Condamine FL, Kuch M, Enk J, Moraes-Barros N, Superina M, Poinar HN, Delsuc F.
715	2016. Shotgun mitogenomics provides a reference phylogenetic framework and timescale for
716	living xenarthrans. <i>Molecular Biology and Evolution</i> 33(3):621–642.
717	
718	Hallgrímsson B, Hall BK. 2005. Variation and variability: central concepts in biology. In:
719	Hallgrímsson B, Hall BK, eds. Variation: A central concept in Biology. Cambridge: Elsevier
720	Academic Press, 1-7.
721	
722	Hamlett GWD. 1939. Identity of Dasypus septemcinctus Linnaeus with notes on some related
723	species. Journal of Mammalogy 20:328-336.
724	
725	Hooper ET. 1947. Notes on Mexican mammals. Journal of Mammalogy 28:40.
726	
727	Huchon D, Delsuc F, Catzeflis FM, Douzery EJP. 1999. Armadillos exhibit less genetic
728	polymorphism in North America than in South America: nuclear and mitochondrial data confirm
729	a founder effect in <i>Dasypus novemcinctus</i> (Xenarthra). <i>Molecular Ecology</i> 8:1743–1748.





730	
731	Ito T, Nishimura TD. 2016. Enigmatic diversity of the maxillary sinus in macaques and its
732	possible role as a spatial compromise in craniofacial modifications. Evolutionary Biology
733	43:414–426.
734	
735	Ito T, Kawamoto Y, Hamada Y, Nishimura TD. 2015. Maxillary sinus variation in hybrid
736	macaques: implications for the genetic basis of craniofacial pneumatization. Biological
737	Journal of the Linnean Society 115(2):333–347.
738	
739	Kim DI, Lee U, Park SO, Kwak DS, Han SH. 2013. Identification Using Frontal Sinus by
740	Three-Dimensional Reconstruction from Computed Tomography. <i>Journal of Forensic Sciences</i>
741	58(1):5-12.
742	
743	Klingenberg CP. 2010. Evolution and development of shape: integrating quantitative approaches
744	Nature Reviews Genetics 11(9):623-635.
745	
746	Krentzel D, Angielczyk K. 2016. Evolution, development and function of the elaborate frontal
747	sinuses in porcupines. The Anatomical Record 299:148.
748	
749	Lönnberg E. 1913. Mammals from Ecuador and related forms. <i>Arkiv för Zoologi</i> 8:1-36.
750	





751	Maier W. 2000. Ontogeny of the nasal capsule in cercopithecoids: a contribution to the
752	comparative and evolutionary morphology of catarrhines. In: Whitehead PF, Jolly CJ, eds. Old
753	World Monkeys. Cambridge: University Press, 99–132.
754	
755	Maier W, Ruf I. 2014. Morphology of the nasal capsule of Primates – with special reference to
756	Daubentonia and Homo. The Anatomical Record 297:1985–2006.
757	
758	Macrini TE. 2012. Comparative morphology of the internal nasal skeleton of adult marsupials
759	based on X-ray computed tomography. Bulletin of the American Museum of Natural History
760	365:1-91.
761	
762	Marquez S. 2008. The paranasal sinuses: the last frontier in craniofacial biology. <i>The Anatomica</i>
763	Record 291:1350–1361.
764	
765	McBee K, Baker RJ. 1982. Dasypus novemcinctus. Mammalian Species 162:1-9.
766	
767	McDonough CM, Loughry WJ. 2013. The nine-banded armadillo: a natural history. Norman,
768	OK: University of Oklahoma Press, 323 pp.
769	
770	Mondolfi E. 1968. Descripción de un nuevo armadillo del genero <i>Dasypus</i> de Venezuela
771	(Mammalia - Edentata). Memoria de la sociedad de ciencias naturales La Salle 27:149-167.
772	





//3	Nomina Anatomica Veterinaria, 5th edn. 2005. Hannover, Columbia, Gent, Sapporo: Editorial
774	Committee. Available at: <a href="http://www.wava-amav.org/downloads/nav_2005.pdf">http://www.wava-amav.org/downloads/nav_2005.pdf</a> .
775	
776	Novacek MJ. 1993. Patterns of diversity in the mammalian skull. In: Hanken J, Hall BK, eds.
777	The Skull, Volume 2: Patterns of Structural and Systematic Diversity. Chicago: University of
778	Chicago Press, pp. 438-545.
779	
780	Paulli S. 1900a. Über die Pneumaticität des Schädels bei den Säugerthieren. Eine
781	morphologische Studie. II. Über die Morphologie des Siebbeins und die der Pneumaticität bei
782	den Ungulaten und Probosciden. Gegenbaurs Morphologisches Jahrbuch 28:179–251.
783	
784	Paulli S. 1900b. Über die Pneumaticität des Schädels bei den Säugerthieren. Eine
785	morphologische Studie. III. Über die Morphologie des Siebbeins und die der Pneumaticität bei
786	den Insectivoren, Hyracoideen, Chiropteren, Carnivoren, Pinnipedien, Edentaten, Rodentiern,
787	Prosimiern und Primaten. Gegenbaurs Morphologisches Jahrbuch 28:483-564.
788	
789	Peters W. 1864. Ueber neue Arten der Saugethier-gattungen Geomys, Haplodon und Dasypus.
790	Monatsbericht der Königlich-Preussischen Akademie der Wissenschaften zu Berlin 1865: 177-
91	181.
792	
793	Rossie JB. 2006. Ontogeny and homology of the paranasal sinuses in Platyrrhini (Mammalia:
794	Primates). Journal of Morphology 267:1–40.
795	





796	Rossie JB. 2008. The phylogenetic significance of anthropoid paranasal sinuses. <i>The Anatomical</i>
797	Record 291:1485–1498.
798	
799	Ruf I. 2014. Comparative anatomy and systematic implications of the turbinal skeleton in
300	Lagomorpha (Mammalia). The Anatomical Record 297:2031–2046.
301	
302	Russell RJ. 1953. Description of a new armadillo (Dasypus novemcinctus) from Mexico with
303	remarks on geographic variation of the species. Proceedings of the Biological Society of
304	Washington 66:21.
305	
306	Sharp AC. 2016. A quantitative comparative analysis of the size of the frontoparietal sinuses and
307	brain in vombatiform marsupials. <i>Memoirs of Museum Victoria</i> 74:331–342.
808	
309	Slavec ZZ. 2005. Identification of family relationships by epigenetic traits. <i>Anthropologischer</i>
310	Anzeiger 63(4):401-408.
311	
312	Soares da Silva AB, de Sousa Cavalcante MMA, Araújo JVS, de Oliveira IM, Fonseca CMB,
313	dos Santos Rizzo M, de Carvalho MAM, Júnior AMC. 2016. Anatomy of the nasal cavity of
314	nine-banded armadillo (Dasypus novemcinctus, Linnaeus, 1758). Jornal Interdisciplinar de
315	Biociências 1:1-4.
316	





817	Szilvássy J. 1982. Zur Variation, Entwicklung und Vererbung der Stirnhöhlen. <i>Annalen des</i>
818	Naturhistorischen Museums in Wien. Serie A für Mineralogie undPetrographie, Geologie und
819	Paläontologie, Anthropologie und Prähistorie, 84:97-125.
820	
821	Tanner JB, Dumont ER, Sakai ST, Lundrigan BL, Holekamp KE. 2008. Of arcs and vaults: the
822	biomechanics of bonecracking in spotted hyenas (Crocuta crocuta). Biological Journal of the
823	Linnean Society 95:246–255.
824	
825	Van Valen L. 1962. A study of fluctuating asymmetry. <i>Evolution</i> 16(2):125-142.
826	
827	Van Valkenburgh B, Smith TD, Craven BA. 2014. Tour of a labyrinth: exploring the vertebrate
828	nose. The Anatomical Record 297:1975–1984.
829	
830	Weidenreich F. 1941. The brain and its role in the phylogenetic transformation of the human
831	skull. Transactions of the American Philosophical Society 31:320–442.
832	
833	Wetzel RM, Gardner AL, Redford KH, Eisenberg JF. 2008. Order Cingulata Illiger, 1811. In:
834	Gardner AL, ed. Mammals of South America, volume 1: marsupials, xenarthrans, shrews and
835	bats. Chicago: University of Chicago Press, pp. 128-157.
836	
837	Wible JR, Gaudin TJ. 2004. On the cranial osteology of the yellow armadillo Euphractus
838	sexcinctus (Dasypodidae, Xenarthra, Placentalia). Annals of Carneggie Museum 73(3):117-196.
839	





840	Witmer LM. 1999. The Phylogenetic History of Paranasal Air Sinuses. In: Koppe T, Nagai H,
841	Alt KW, eds. The paranasal sinuses of higher primates: development, function and evolution.
842	Berlin: Quintessence, pp. 21-34.
843	
844	Zollikofer CPE, Weissmann JD. 2008. A morphogenetic model of cranial pneumatization based
845	on the invasive tissue hypothesis. <i>The Anatomical Record</i> 291:1446–1454.
846	
847	Zuckerkandl E. 1887. Das periphere Geruchsorgan der Säugethiere: eine vergleichend
848	anatomische Studie. Whitefish: Kessinger Publishing, 146pp.
849	
850	
851	
852	Figure legends
	Figure legends  Figure 1. Dorsal views of virtually reconstructed skulls of long-nosed armadillos species, with
853	
853 854	Figure 1. Dorsal views of virtually reconstructed skulls of long-nosed armadillos species, with
853 854 855	<b>Figure 1</b> . Dorsal views of virtually reconstructed skulls of long-nosed armadillos species, with bone transparency showing internal paranasal sinuses and recesses in light blue. See Material and
853 854 855 856	<b>Figure 1</b> . Dorsal views of virtually reconstructed skulls of long-nosed armadillos species, with bone transparency showing internal paranasal sinuses and recesses in light blue. See Material and
853 854 855 856 857	<b>Figure 1</b> . Dorsal views of virtually reconstructed skulls of long-nosed armadillos species, with bone transparency showing internal paranasal sinuses and recesses in light blue. See Material and Methods for the abbreviations. Scale-bar: 10mm.
853 854 855 856 857 858	Figure 1. Dorsal views of virtually reconstructed skulls of long-nosed armadillos species, with bone transparency showing internal paranasal sinuses and recesses in light blue. See Material and Methods for the abbreviations. Scale-bar: 10mm.  Figure 2. Paranasal sinuses and recesses in juvenile individuals of <i>Dasypus novemcinctus</i> ,
852 853 854 855 856 857 858 859	Figure 1. Dorsal views of virtually reconstructed skulls of long-nosed armadillos species, with bone transparency showing internal paranasal sinuses and recesses in light blue. See Material and Methods for the abbreviations. Scale-bar: 10mm.  Figure 2. Paranasal sinuses and recesses in juvenile individuals of <i>Dasypus novemcinctus</i> , virtual reconstructions of skulls in lateral and dorsal views (left and right sides of the figure
853 854 855 856 857 858	Figure 1. Dorsal views of virtually reconstructed skulls of long-nosed armadillos species, with bone transparency showing internal paranasal sinuses and recesses in light blue. See Material and Methods for the abbreviations. Scale-bar: 10mm.  Figure 2. Paranasal sinuses and recesses in juvenile individuals of <i>Dasypus novemcinctus</i> , virtual reconstructions of skulls in lateral and dorsal views (left and right sides of the figure respectively), with and without bone transparency. See Material and Methods for the



<b>Figure 3.</b> Virtual reconstruction of the skull of the stillborn specimen AMNH 33150, <i>Dasypus</i>
novemcinctus, with bone transparency leaving the caudal maxillary recess and cavity for the
frontal diploic vein apparent. Top, dorsal view; bottom, lateral view.
Figure 4. Dorsal views of virtually reconstructed skulls of <i>Dasypus novemcinctus</i> clustered by
morphotypes of paranasal anatomy as described in the text. Bone transparency leaves apparent
the paranasal recesses and sinuses in light blue. Scale bar: 10 mm.
Figure 5. Computed-tomography transversal slices through the skull of <i>D. novemcinctus</i>
individuals showing details of the internal paranasal anatomy for each morphotype. Slices were
made at similar transversal locations at the posterior end of the anterior root of the zygomatic
arch. See Material and Methods for the abbreviations. Scale-bar: 10mm.
aton, soo material and monoto for the accretiations, source our, romain.
and in see Francisca for the accreviations. Seale call formin.
Figure 6. Summary map showing the geographical distribution of nine-banded armadillo
Figure 6. Summary map showing the geographical distribution of nine-banded armadillo
<b>Figure 6.</b> Summary map showing the geographical distribution of nine-banded armadillo specimens investigated in this study and their attribution to a paranasal morphotype. Each of the
<b>Figure 6.</b> Summary map showing the geographical distribution of nine-banded armadillo specimens investigated in this study and their attribution to a paranasal morphotype. Each of the morphotype is represented by a schematic dorsal view of skulls (in grey) on which the paranasal
<b>Figure 6.</b> Summary map showing the geographical distribution of nine-banded armadillo specimens investigated in this study and their attribution to a paranasal morphotype. Each of the morphotype is represented by a schematic dorsal view of skulls (in grey) on which the paranasal sinuses and recesses are drawn (in blue, yellow, or green for each morphotype). Specimens
<b>Figure 6.</b> Summary map showing the geographical distribution of nine-banded armadillo specimens investigated in this study and their attribution to a paranasal morphotype. Each of the morphotype is represented by a schematic dorsal view of skulls (in grey) on which the paranasal sinuses and recesses are drawn (in blue, yellow, or green for each morphotype). Specimens
<b>Figure 6.</b> Summary map showing the geographical distribution of nine-banded armadillo specimens investigated in this study and their attribution to a paranasal morphotype. Each of the morphotype is represented by a schematic dorsal view of skulls (in grey) on which the paranasal sinuses and recesses are drawn (in blue, yellow, or green for each morphotype). Specimens
<b>Figure 6.</b> Summary map showing the geographical distribution of nine-banded armadillo specimens investigated in this study and their attribution to a paranasal morphotype. Each of the morphotype is represented by a schematic dorsal view of skulls (in grey) on which the paranasal sinuses and recesses are drawn (in blue, yellow, or green for each morphotype). Specimens



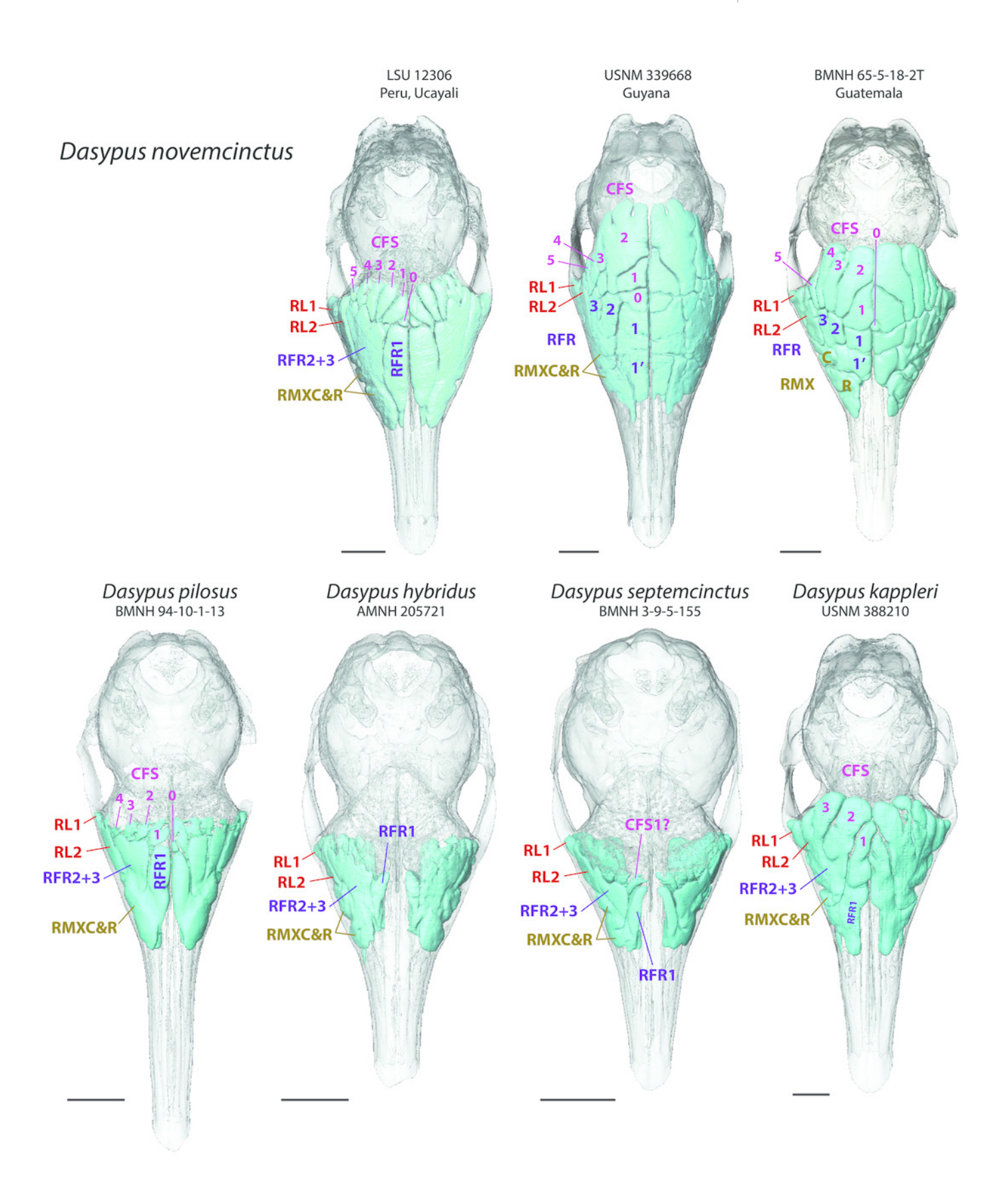


885	
886	Supplemental Table S1. Table with information on investigated specimens: taxa, geographical
887	origins, collection number, scan details, sinus morphotypes.
888	
889	Supplemental Figure S2. Illustration of the paranasal sinuses and recesses in different specimens
890	of Dasypus kappleri, with geographical information. Skulls not to scale.



Dorsal views of virtually reconstructed skulls of long-nosed armadillos species, with bone transparency showing internal paranasal sinuses and recesses in light blue.

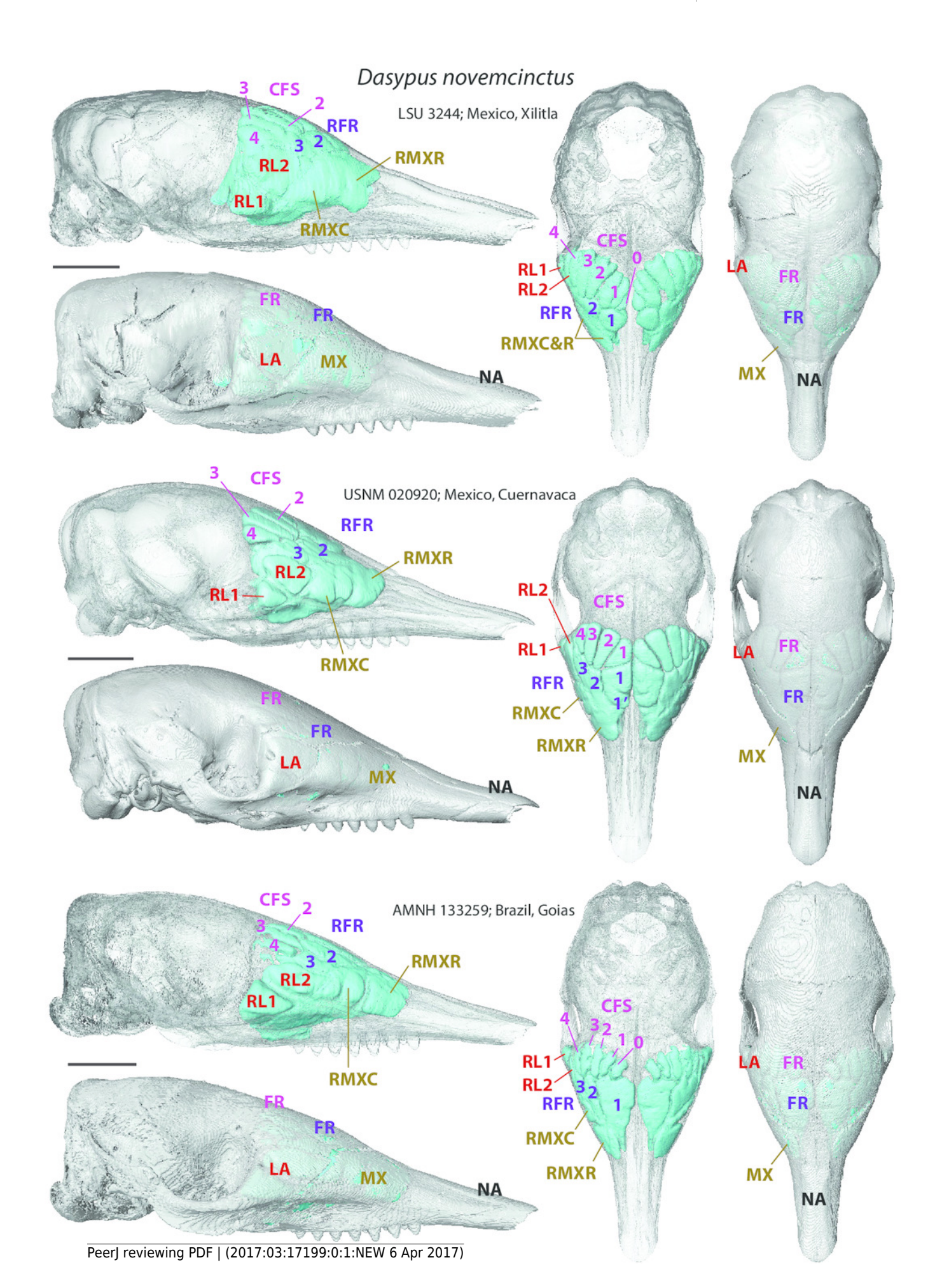
**Figure 1**. Dorsal views of virtually reconstructed skulls of long-nosed armadillos species, with bone transparency showing internal paranasal sinuses and recesses in light blue. See Material and Methods for the abbreviations. Scale-bar: 10mm.





Paranasal sinuses and recesses in juvenile individuals of *Dasypus novemcinctus* 

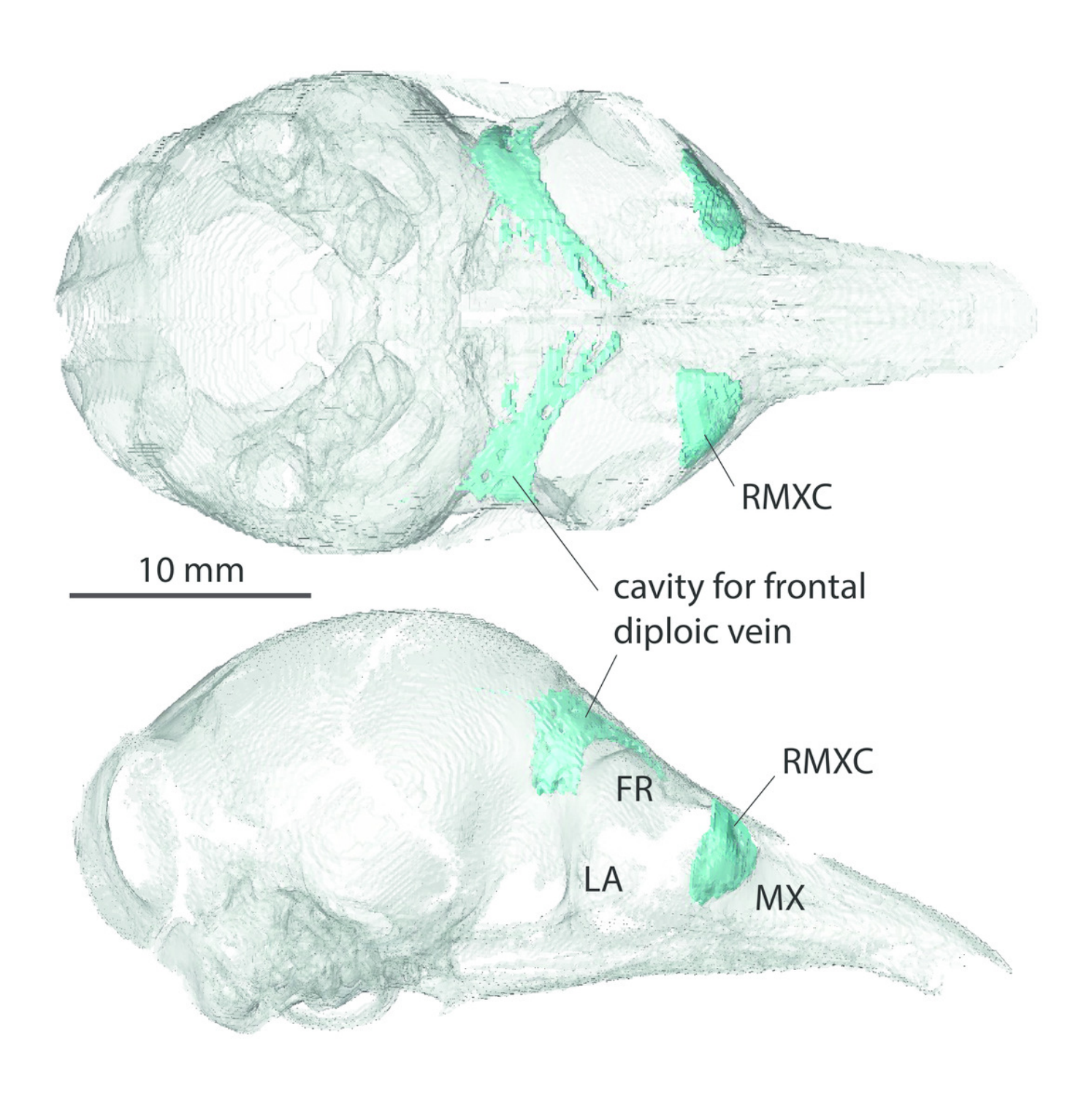
**Figure 2.** Paranasal sinuses and recesses in juvenile individuals of *Dasypus novemcinctus*, virtual reconstructions of skulls in lateral and dorsal views (left and right sides of the figure respectively), with and without bone transparency. See Material and Methods for the abbreviations. Scale-bar: 10mm.





Virtual reconstruction of the skull of the stillborn specimen AMNH 33150, *Dasypus novemcinctus* 

**Figure 3.** Virtual reconstruction of the skull of the stillborn specimen AMNH 33150, *Dasypus novemcinctus*, with bone transparency leaving the caudal maxillary recess and cavity for the frontal diploic vein apparent. Top, dorsal view; bottom, lateral view.



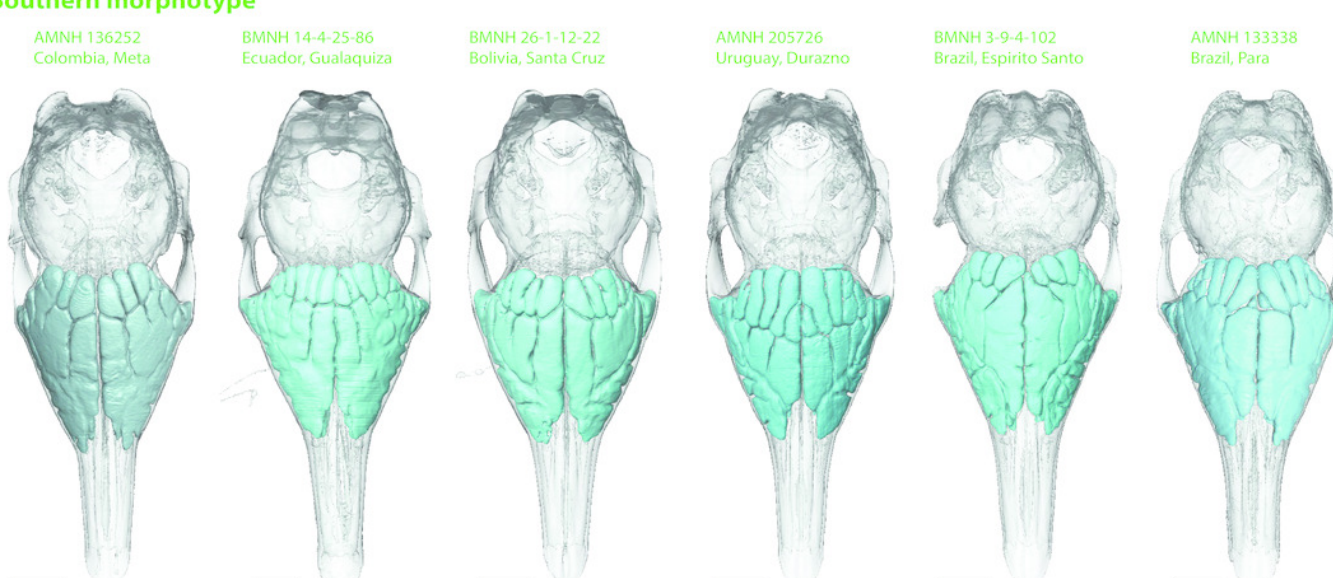


Dorsal views of virtually reconstructed skulls of *Dasypus novemcinctus* clustered by morphotypes

**Figure 4.** Dorsal views of virtually reconstructed skulls of *Dasypus novemcinctus* clustered by morphotypes of paranasal anatomy as described in the text. Bone transparency leaves apparent the paranasal recesses and sinuses in light blue. Scale bar: 10 mm.

### **PeerJ**

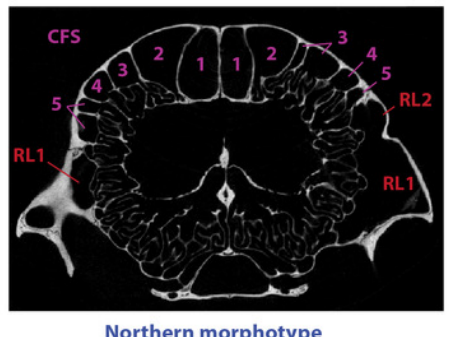
# Northern morphotype LSU 29160 USA, Mississipi USA, Louisiana Mexico, Sinaloa Mexico, Sinaloa Nicaragua LSU 15762 Costa Rica Ecuador, El Oro Southern morphotype AMNH 136252 Colombia, Meta BMNH 14-4-25-86 Ecuador, Gualiaguiza BMNH 26-1-12-22 Bolivía, Santa Cruz AMNH 205726 Uruguay, Durazno Brazil, Espirito Santo Brazil, Espirito Santo Brazil, Espirito Santo



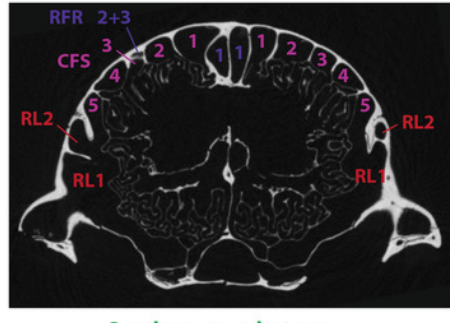


Computed-tomography transversal slices through the skull of D. novemcinctus individuals showing details of the internal paranasal anatomy

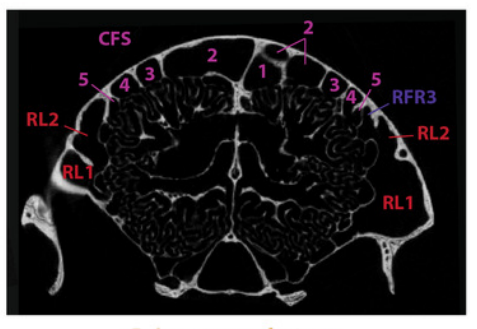
Figure 5. Computed-tomography transversal slices through the skull of D. novemcinctus individuals showing details of the internal paranasal anatomy for each morphotype. Slices were made at similar transversal locations at the posterior end of the anterior root of the zygomatic arch. See Material and Methods for the abbreviations. Scale-bar: 10mm.







**Southern morphotype** BMNH 3-9-4-102



Guianan morphotype AP 207



Summary map showing the geographical distribution of nine-banded armadillo specimens investigated in this study and their attribution to a paranasal morphotype

**Figure 6.** Summary map showing the geographical distribution of nine-banded armadillo specimens investigated in this study and their attribution to a paranasal morphotype. Each of the morphotype is represented by a schematic dorsal view of skulls (in grey) on which the paranasal sinuses and recesses are drawn (in blue, yellow, or green for each morphotype). Specimens reported with a star denote the absence of geographical information besides the country of origin.



